SPATIAL DISTRIBUTIONS OF A3558 IN THE CORE REGION OF THE SHAPLEY SUPERCLUSTER

F. AKIMOTO, K. KONDOU, A. FURUZAWA, Y. TAWARA, AND K. YAMASHITA

Department of Physics, Nagoya University, Furo-cho, Chikusa-ku, Nagoya 464-8602, Japan

Received 2002 November 27; accepted 2003 June 19

ABSTRACT

The core region of the Shapley supercluster is dominated by three rich Abell clusters and two poor clusters. Since these member clusters are expected to be evolving rapidly in comparison to nonmember clusters because of the high merging rate, it is important to study the member clusters for understanding of the cluster evolution. Since the spatial distributions of gas temperature and metal abundance in each member cluster provide us with information on the interactions and motions of member clusters, they are useful for understanding their dynamics. From the results of eight *ASCA* pointing observations (total ∼300 ks) of the core region, we obtained parameters of gas temperature, metal abundance, and X-ray luminosity for five member clusters and found that they are similar to the other field clusters not belonging to superclusters observed with *ASCA*. This result and the mean gravitational mass density of the core region indicate that the members are growing in the same way as the nonmember clusters, and the core of the supercluster is just on the way to contraction. Based on analyses of detailed spatial structures with a $4' \times 4'$ scale, the two poor clusters show nearly isotropic temperature distributions, while the three Abell clusters are asymmetric. A3558 was analyzed with a $2' \times 2'$ scale, owing to the statistical advantage, and it was revealed that A3558 has clear asymmetric distributions of gas temperature and X-ray surface brightness. This is thought to be caused by cluster-cluster mergings and/or group infallings. A metal-rich region with the size of ∼320 h_{50}^{-1} kpc was also found to the southeast, ∼12′ away from the cluster center of A3558. It is expected that either a remnant of a merged core has been left after a major merging or a group of galaxies has been recently infalling. Thus, the high dynamical activity of A3558 is proved.

Subject headings: galaxies: clusters: individual (A3558) — X-rays: galaxies: clusters

1. INTRODUCTION

Superclusters have the highest number density of galaxy clusters in the universe. Compared to field galaxy clusters, the member clusters in a supercluster are thought to merge easily with each other, or with galaxies and groups of galaxies within the potential well of the supercluster. Thus, the dynamical state of supercluster members is a clue to interpreting the evolution of large-scale structures in the universe.

The Shapley supercluster, SCL 124 (Einasto et al. 1997), has 25 Abell clusters of galaxies within a radius of 50 h_{50}^{-1} Mpc and is the region with the highest known number density of member clusters. In particular, the core region of the Shapley supercluster is defined to be a region lying east to west over 15 h_{50}^{-1} Mpc (Bardelli et al. 1998) that contains five clusters of galaxies. Easternmost are A3562, SC 1329−313, and SC 1327−312, A3558 is in the center position, and westernmost is A3556, as shown in Figure 1.

Since the core region was observed in the optical wavelength by Shapley (1930), many multiwavelength observations have been done. The radial velocity and distribution of the galaxies have been investigated with optical observations in detail (Bardelli et al. 1998, 2000). X-ray observations have also been done by various satellites: *Ginga* (Day et al. 1991), *Einstein* (Raychaudhury et al. 1991; Breen et al. 1994), *ROSAT* (Ettori, Fabian, & White 1997; Ettori et al. 2000), and *ASCA* (Markevitch & Vikhlinin 1997 for A3558; Hanami et al. 1999 for the five core members). The temperature distributions of A3558 and SC 1329−313 were investigated by Markevitch & Vikhlinin (1997) and Hanami et al. (1999), respectively, and they reported asymmetric distributions. The total gravitational mass of the core region is esti-

mated to be 10^{15}–10^{16} h_{50}^{-1} $M_\odot$ from galaxy radial velocity dispersion (Metcalfe, Godwin, & Peach 1994) and X-ray observation (Raychaudhury et al. 1991; Ettori et al. 1997).

The central galaxy cluster in the core region of the Shapley supercluster, A3558, is one of the richest clusters of galaxies. Observational results in the X-ray band of A3558 estimate the gas temperature of the overall region to be 3–4 keV (Bardelli et al. 1996) with *ROSAT* and 5–6 keV (Day et al. 1991; Markevitch & Vikhlinin 1997; Hanami et al. 1999) with *Ginga* and *ASCA*. There is a difference among the satellites because of the limitation of the observable energy band. The metal abundance and gravitational mass of A3558 are estimated to be ∼0.3 solar (Day et al. 1991; Bardelli et al. 1996; Hanami et al. 1999) and $(3$–$6) \times 10^{14}$ h_{50}^{-1} $M_\odot$ (Bardelli et al. 1996; Ettori et al. 1997), respectively. The temperature and abundance of the whole region are typical values for a galaxy cluster.

A3558 has a galaxy density distribution elongated in the northwest-southeast direction, and many groups and clusters of galaxies are aligned along this major axis (Bardelli et al. 1994). The X-ray surface brightness distribution also elongates in the same direction (Bardelli et al. 1996). Therefore, in this core region of the Shapley supercluster, the infall of matter along this axis is thought to be dominant. From these characteristics and the two-dimensional distributions of gas temperature and metal abundance obtained by *ASCA* observations, we discuss the dynamical structure of A3558.

This paper comprises six sections: In § 2 the details of the *ASCA* observations and analysis method are described. We present the results of the *ASCA* data analysis for A3558 in § 3 and for other member clusters of the Shapley core in § 4. In § 5 the resulting two-dimensional distributions of X-ray
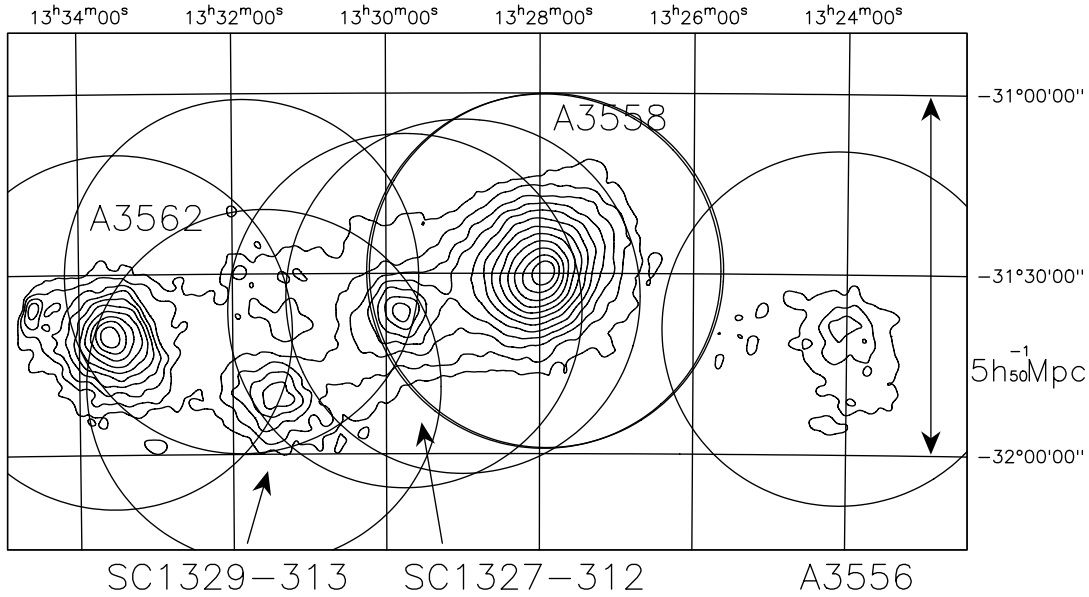
Fig. 1.—*ASCA* image of the core region in the Shapley supercluster. The energy band is 0.7–10 keV. The circles show *ASCA* fields of view. The adopted equinox year is J2000.0.

surface brightness, gas temperature, and metal abundance are discussed, and finally, in § 6 a summary of our work is provided. Throughout this paper we use the solar abundance table given by Anders & Grevesse (1989), $H_0 = 50$ km s^{-1} Mpc^{-1}, and $q_0 = 0$, and the quoted errors of the spectral parameters are at the 90% confidence level.

2. OBSERVATIONS

Eight points in the core region of the Shapley supercluster were observed with *ASCA*. The longest observation among these pointings was done for A3558, which is the brightest X-ray source among the five targets in the core. In this paper we present the results of a detailed study of this target. Data from the other four X-ray sources are also analyzed with the same method. The observational log of these data is shown in Table 1. Hanami et al. (1999) and Markevitch & Vikhlinin (1997) have already reported the results of analyses for the core without the additional observation of A3558 (observation 8 in Table 1).

We analyzed *ASCA* data using LHEASOFT, version 5.0.1, supplied by the NASA Goddard Space Flight Center. After data screening with the standard criterion, a rise-time discrimination technique was applied for data of the Gas Imaging Spectrometer (GIS) to reject particle events and a *sisclean* for data of the Solid-State Imaging Spectrometer (SIS) to exclude hot pixels. We estimated backgrounds from point-source–removed data of GIS blank-sky files[1] and standard data (1994 November) of SIS blank-sky files.

[1] See http://heasarc.gsfc.nasa.gov/docs/asca/mkgisbgd/mkgisbgd.html.

TABLE 1
LOG OF *ASCA* OBSERVATIONS

| NUMBER | TARGET NAME | OBSERVED DATE | EXPOSURE (ks) | | POSITION (J2000.0) | |
			GIS	SIS[a]	α	δ
1........................	A3558	1994 Jul 14–15	20.8	20.4♠	13 27 56.9	−31 29 38.4
2........................	A3556	1995 Jan 23–24	39.1	39.9♠	13 24 06.0	−31 38 60.0
3........................	SC 1327−312	1995 Jan 24–25	30.4	29.4◇	13 29 45.4	−31 36 11.9
4........................	IC region[b]	1995 Jul 23–24	31.9	30.8◇	13 29 00.0	−31 33 50.0
5........................	A3562	1996 Jul 27	19.8	20.2◇	13 33 31.8	−31 39 36.0
6........................	SC region[c]	1996 Jul 27–29	45.0	44.9◇	13 31 52.8	−31 30 25.2
7........................	SC 1329−313	1996 Jul 29	27.7	28.5◇	13 31 35.9	−31 48 44.6
8........................	A3558	2000 Jan 21–24	71.7	66.5♣	13 27 54.8	−31 29 31.9

NOTES.—Units of right ascension are hours, minutes, and seconds, and units of declination are degrees, arcminutes, and arcseconds. We used three pointing data from observations 1, 4, and 8 for our investigation of A3558.

[a] Here spade (♠) symbols are for the 4 CCD mode, diamonds (◇) for the 2 CCD mode, and clubs (♣) for the 1 CCD mode.

[b] The midpoint between A3558 and SC 1327−312.

[c] Off-center region near A3562, SC 1329−313, and SC 1327−312.

3. RESULTS OF THE *ASCA* DATA ANALYSIS OF A3558

A3558, located at the center of the Shapley supercluster core, has been observed three times with *ASCA* (observations 1, 4, and 8 in Table 1). The total exposure time of these observations is 120 ks for each GIS detector, and the total number of photons within a radius of $12'$ ($\sim 1\ h_{50}^{-1}$ Mpc) is 1.6×10^5 counts per detector.

Figure 2 shows an X-ray image obtained by these *ASCA* GIS observations. After the background subtraction, a correction of surface brightness was done using the exposure map and GIS detector efficiency map. The central X-ray peak in Figure 2 coincides with A3558, and the east peak is a poor cluster, SC 1327−312. X-ray energy spectra of GISs within a radius of $12'$ ($\sim 1\ h_{50}^{-1}$ Mpc) at the center of A3558 were evaluated with an absorbed thermal (Raymond-Smith) model. The flux-weighted gas temperature and abundance are estimated to be 5.59 ± 0.06 keV and 0.34 ± 0.02 solar, respectively. The 2–10 keV luminosity is $(6.8 \pm 0.5) \times 10^{44}\ h_{50}^{-2}$ ergs s^{-1}. The redshift and galactic hydrogen column density for absorption are fixed at 0.0482 (Abell, Corwin, & Olowin 1989) and 3.89×10^{20} cm^{-2} (Dickey & Lockman 1990), respectively. The spectral parameters obtained from *ASCA* GIS and SIS data are consistent within a 90% confidence level.

As seen in the *ROSAT* image, *ASCA* also shows that the X-ray surface brightness distribution of A3558 is elongated in the northwest-southeast direction, even in the higher energy band. This structure is thought to be observational evidence that a cluster merging has already happened in A3558 one or more times. In order to confirm this scenario and investigate the physical processes in detail, two-dimensional distributions of temperature and abundance were made. These maps are powerful tools for understanding the dynamical activity and evolution of the galaxy cluster.
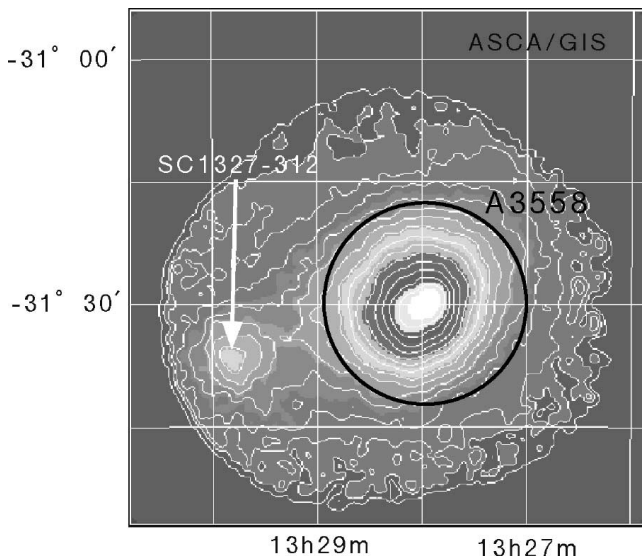
3.1. *Assessment of the Merging Effect in Temperature and Abundance Maps*

The merging process distorts not only the distribution of the X-ray surface brightness but also the distributions of temperature and abundance. Some authors have already revealed azimuthally asymmetric temperature maps, even for clusters with symmetric surface brightness distribution, which had been thought to have been isolated for a long time (Watanabe et al. 1999). It takes typically several giga-years to smooth the X-ray surface brightness, although it depends on the mass ratio of the clusters or the impact parameter of the merging. On the other hand, the distributions of temperature and abundance can keep information about the merging longer than that of surface brightness. Therefore, temperature and abundance maps are very important for studying a merger history. We derived the distributions of the temperature and abundance of A3558 by using some hardness ratio maps. A detailed description of the method is below.

A hardness ratio is an indicator of gas temperature. For an X-ray cluster with a temperature of 5.59 keV, the hardness ratio of the 2.5–10 keV energy band (the hard band) to the 0.7–2.5 keV energy band (the soft band) is ~ 0.57 in the case of the *ASCA* GIS. After background subtraction, a two-dimensional hardness ratio plot was made by dividing the hard-band image by the soft-band image with an angular resolution of $2' \times 2'$. This map shows that the gradient of the hardness ratio coincides with the direction of the major axis of the X-ray surface brightness of A3558. The hardness ratio map is peaked at $\sim 4'$ northwest from the central region of A3558 and decreases in the northwest and southeast directions.

A two-dimensional temperature map is obtained from the hardness ratio map in the following way: Assuming isothermal spherical symmetry of the surface brightness, which is fitted by a single β-model with parameters of a core radius of 4.2 and β of 0.611 from Bardelli et al. (1996), hardness ratio maps are simulated using an *ASCA* full simulation program at a given temperature from 3.5 to 7.5 keV with a step of 0.1 keV. From these maps, the relation between the simulated hardness ratio and the assumed temperature at each position on the detectors is derived. The hardness ratio map is converted according to this relation into a temperature map. An estimated temperature map within the radius of $12'$ at the center of A3558 is shown in Figure 3. The superposed contour is an X-ray image in the 0.7–10 keV band, corrected by the exposure map and the *ASCA* GIS detector efficiency map as shown in Figure 2. The error shown in this figure is the largest error of the temperature at 90% confidence within the radius of $12'$. This temperature map also shows the gradient along the major axis of A3558 as seen in the hardness ratio map. The peak value of the temperature map is 6.5 keV at the position of $\sim 4'$ northwest of the center of A3558, and the temperature decreases by ~ 1 keV farther northwest. This map also shows a possible temperature drop in the southeast direction from the cluster center. Although these characteristics are consistent with the result shown by Markevitch & Vikhlinin (1997), our derived temperature map enables us to investigate spatial structure in detail. The derived temperature is ranging mainly over 5.0–6.5 keV. No remarkable high-temperature regions are seen within the radius of $12'$, such as the hot regions with temperatures of over 10 keV seen in typical merging clusters, e.g.,

Fig. 2.—*ASCA* GIS image for the 0.7–10 keV energy band from observations 1, 4, and 8 in Table 1. The radius of the circle is $1\ h_{50}^{-1}$ Mpc (see text for details).
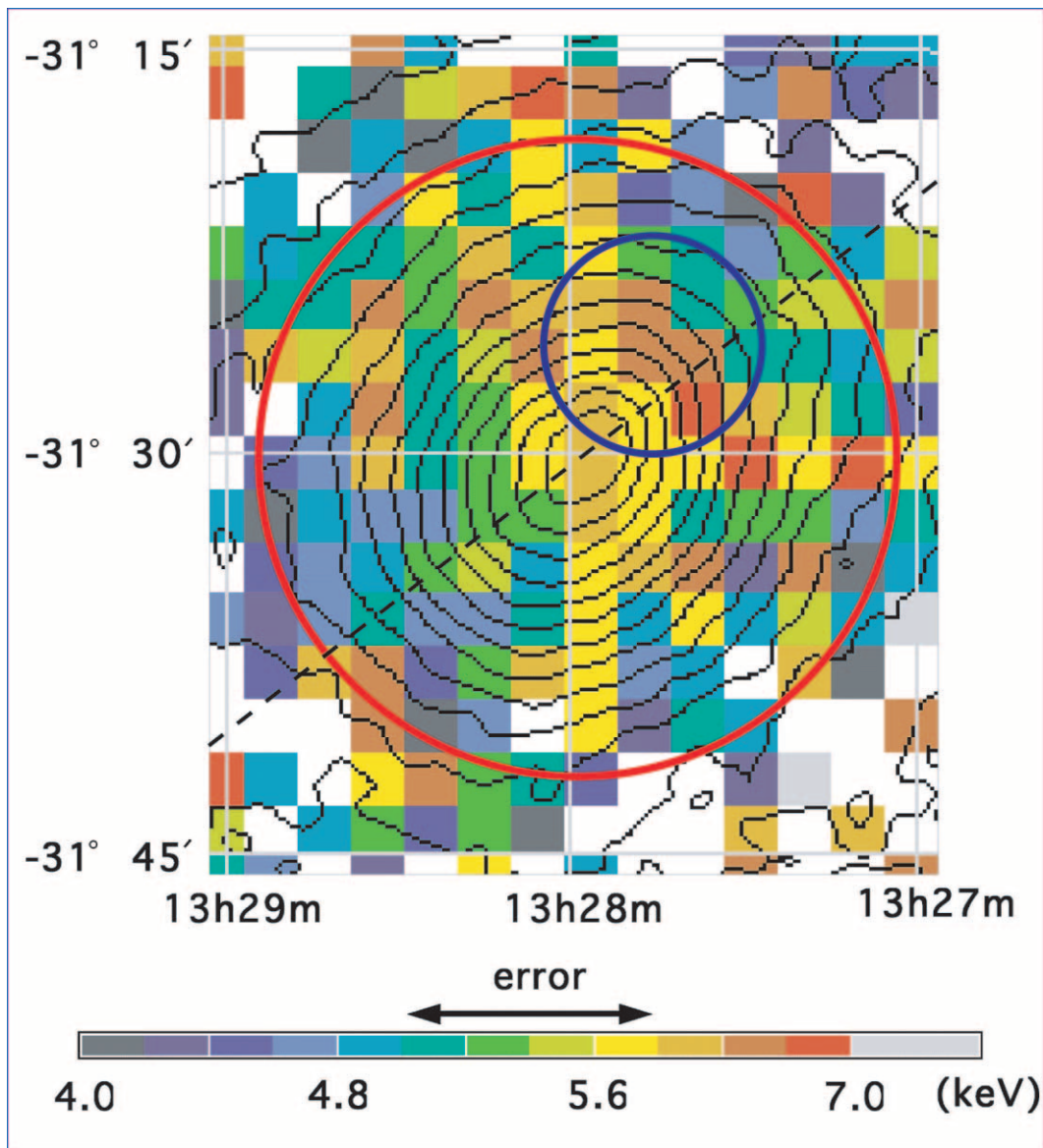
Fig. 3.—*ASCA* temperature map of A3558. The units are keV. The radius of the red circle is 1 h_{50}^{-1} Mpc (=12′), and the dashed line shows the major axis. The superposed contours show the X-ray surface brightness of the 0.7–10 keV energy band. The pixel size is 2′ × 2′. The error shown by the arrow is the maximum error of the temperature within a radius of 12′. The blue circle shows region 1.

the 0.8 h_{50}^{-1} Mpc off-center region of the Coma Cluster (Watanabe et al. 1999) and the 1.0 h_{50}^{-1} Mpc off-center region of the Ophiuchus Cluster (Watanabe et al. 2001). Moreover, there are also no clear, striking low-temperature regions, such as a cool region (cold front) 2 keV lower than the other regions in the merging cluster, e.g., A3667 (Vikhlinin, Markevitch, & Murray 2001) and A2142 (Markevitch et al. 2000), which were revealed by *Chandra* observations.

Because the gravitational settling of heavy elements takes much longer than the age of the universe (Sarazin 1988), the observed abundance map can constrain the amount of mixing due to a small-scale merging or turbulence that can take place in a galaxy cluster. Moreover, even if large-scale cluster-cluster merging has occurred, their abundance distributions have been disturbed by the merging process less effectively than their temperature maps. That is, not only the chemical evolution but also the dynamical evolution can be

revealed from an abundance map. To get a two-dimensional distribution of metal abundance, an intensity ratio of the iron K line and the neighboring continuum emission is estimated. First, images in two energy bands, 5.0–6.0 and 6.0–7.0 keV, are made from *ASCA* data at the spatial resolution of 4′ × 4′. The image of the 5.0–6.0 keV energy band can be safely expected to include only continuum emission. On the other hand, the 6.0–7.0 keV image includes iron lines in addition to the continuum emission. Next, the two images of the 6.0–7.0 keV continuum emission and the 5.0–6.0 keV continuum emission are simulated using the *ASCA* full simulation program. In this simulation, the temperature is assumed to be 6.75 keV, which is obtained from *ASCA* GIS and SIS 4–10 keV spectra within the radius of 4′. The assumed parameters of the β-model are the same as the ones used for estimating the temperature map (Bardelli et al. 1996). From these simulated images, the two-dimensional continuum intensity ratio

map, $f = I_{6-7\,keV}/I_{5-6\,keV}$, is obtained. By multiplying the *ASCA* observed 5.0–6.0 keV image by this ratio map f, we can guess the 6.0–7.0 keV continuum image. An iron-line intensity map is derived by subtracting this estimated continuum image from the *ASCA* observed 6.0–7.0 keV image. Dividing this iron-line map by the simulated 6.0–7.0 keV continuum image gives a ratio map of iron-line intensity to continuum, corresponding to an equivalent-width map. Finally, an abundance map is obtained by normalizing the value averaged within a circle of radius 4′. The obtained abundance map is shown in Figure 4. Although the above described simulation was done on the assumption of isothermal distribution, the nonisothermality mentioned in this section causes an uncertainty of the abundance of ∼10%.

In Figure 4, 4 pixels within the southeast region 12′ away from the center show high abundance, and this is also implied in the south region at same distance from the center, while other regions are almost the same within the error.

3.2. *Detailed Structure of X-Ray Surface Brightness Distribution*

To know the relation of the X-ray surface brightness distribution to some interesting features seen in the temperature and abundance maps, and moreover to get higher order structures of the surface brightness distribution, we investigated the deviation of the X-ray surface brightness from the smooth function described with an elliptical β-model. The 0.7–10 keV *ASCA* image was simulated using the *ASCA* full simulation program, assuming a core radius of 4.′9 and 3.′6, a β of 0.61 (Bardelli et al. 1996), a temperature of 5.8 keV, and an abundance of 0.32 solar. The temperature and abundance were obtained from only the *ASCA* GIS spectrum within a radius of 4′.

By subtracting the simulated image from the observed 0.7–10 keV image, we got substructures as shown in Figure 5. This residual image is shown in units of the brightness fluctuation of the observed 0.7–10 keV image, that is,
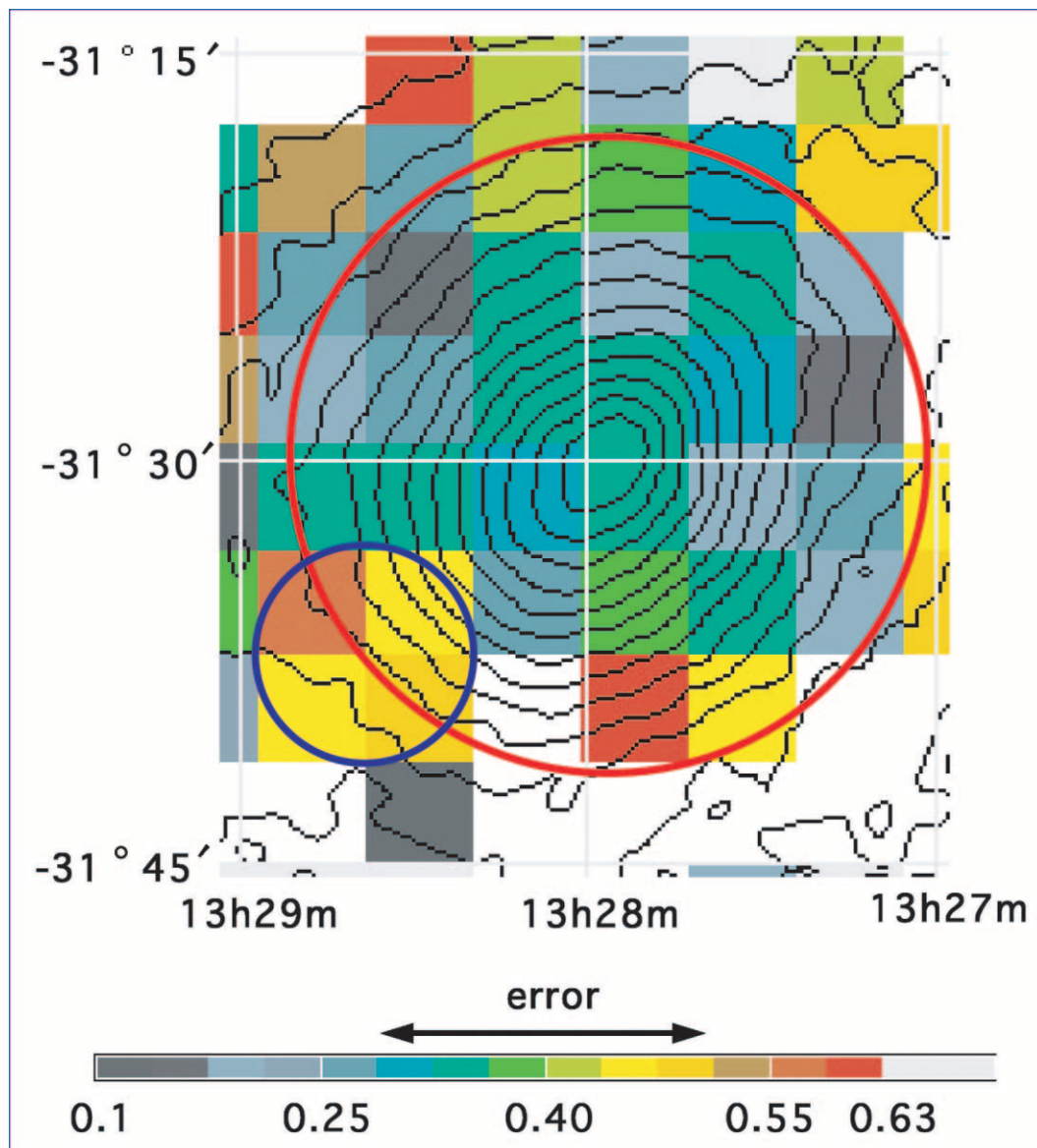
Fɪɢ. 4.—*ASCA* abundance map of A3558. The units are in solar metallicity. The red circle and superposed contour are the same as for Fig. 3. The error shown by the arrow is the maximum error of the abundance within a radius of 12′. The pixel size is 4′ × 4′. The blue circle shows region 3.
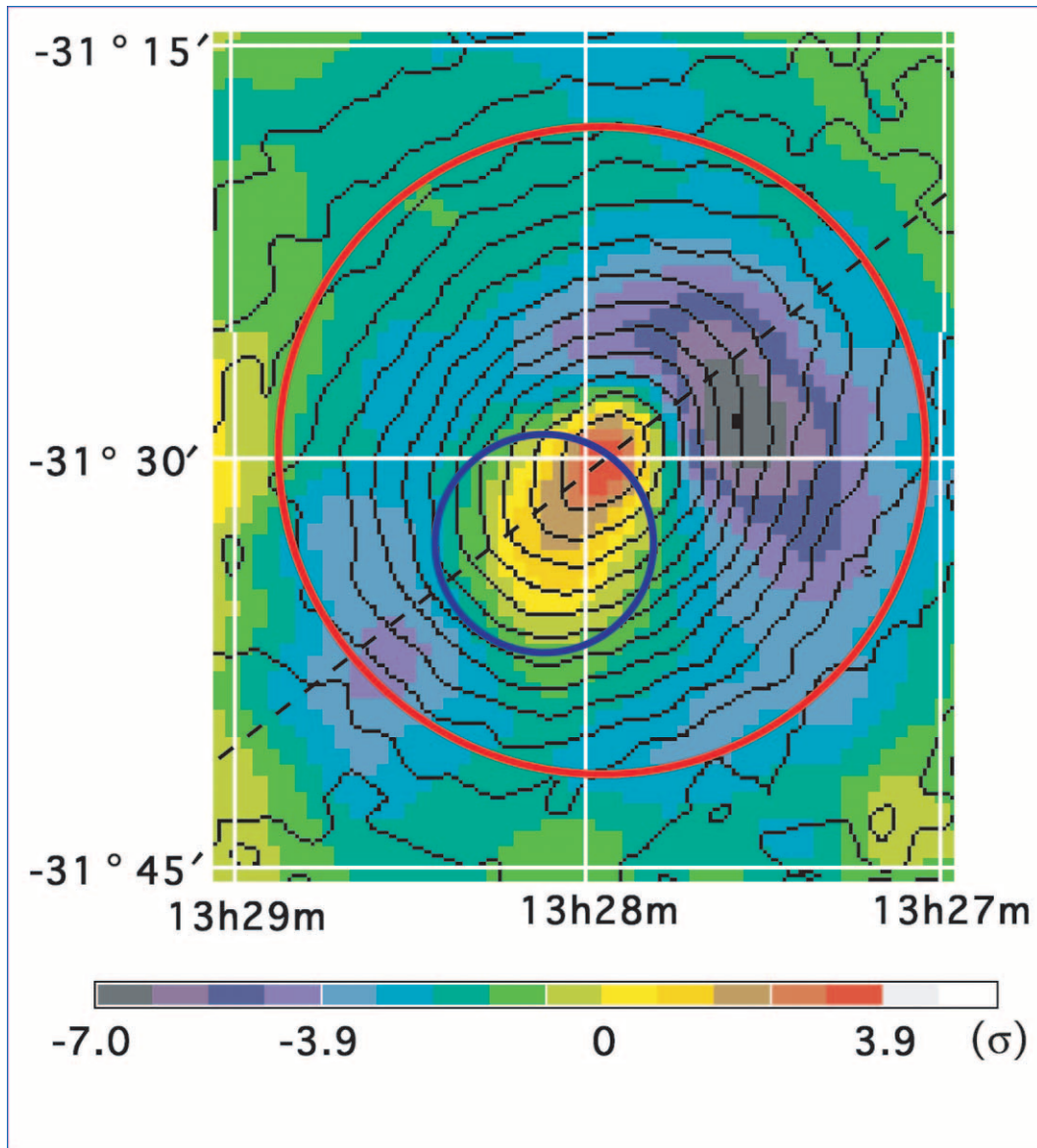
Fig. 5.—*ASCA* residual image of A3558. The units are in σ. The dashed line, red circle, and superposed contour are the same as for Fig. 3. The blue circle shows region 2.

σ. Excess emission over the 3 σ level is seen in the central region and expands to the southeast. On the other hand, there are two drops of over the 3 σ level in regions $\sim 5'$ northwest and $\sim 10'$ southeast along the spheroidal major axis. These structures resemble the sharp edge shown in many merging clusters. The central excess flux within a radius of 2.5 is estimated to be $\sim 9\%$ of the whole cluster. Since there is a dominant galaxy at the center of A3558, corresponding to the central excess region, it can be thought that the excess flux is associated with this galaxy. If it is so, the corresponding luminosity of this excess is estimated to be $1.4 \times 10^{43} \, h_{50}^{-2}$ ergs s^{-1}. The spectrum of this region is well fitted with a single-temperature thermal (Raymond-Smith) model with a temperature of 5.8 ± 0.1 keV and an abundance of 0.35 ± 0.04 solar at the reduced χ^2 of 1.17. Two-temperature model fitting has been done, and the obtained parameters are temperatures of $6.4^{+0.2}_{-0.3}$ and $2.0^{+1.2}_{-0.6}$ keV and an abundance of 0.35 ± 0.04 solar, although the reduced χ^2 value is not improved significantly.

According to a comparison of this residual image with the temperature map and the abundance map, no clear excess has appeared at any regions showing peculiarities in the temperature and abundance maps. On the contrary, in the hot region $\sim 4'$ northwest from the cluster center, the surface brightness decreases. Distributions of surface brightness and temperature in this region resemble those of the cold front in A2142 and A3667 revealed by *Chandra* observation (Markevitch et al. 2000; Vikhlinin et al. 2001), which is thought to be a boundary of the remaining core of the merger component, moving through the hotter ambient intracluster medium. Their hot faint regions have cold fronts that lie close to the center of these clusters, because the core has already passed through the central region of another merged cluster.

3.3. *Peculiar Regions within A3558*

As described in §§ 3.1 and 3.2, peculiar regions in the spatial distributions of temperature, abundance, and residual

TABLE 2

POSITION AND X-RAY SPECTRAL PARAMETERS

	POSITION (J2000.0)			SPECTRAL PARAMETERS	
REGION	α	δ	CHARACTERISTICS	kT (keV)	Abundance (Solar)
1......................	13 27 46.4	−31 26 03	High temperature, depression	6.12 ± 0.18	0.32 ± 0.04
2......................	13 28 05.5	−31 33 02	Excess emission	$5.51^{+0.10}_{-0.09}$	0.33 ± 0.03
3......................	13 28 37.8	−31 37 27	Metal-rich	$5.17^{+0.27}_{-0.26}$	0.58 ± 0.11

NOTES.—Units of right ascension are hours, minutes, and seconds, and units of declination are degrees, arcminutes, and arcseconds. The radii of these regions are 4′, and their redshift and absorption are fixed at 0.0482 and 3.89×10^{20} cm^{-2}, respectively.

X-ray surface brightness are detected. To study these regions in detail by spectra, we define three circular regions with a radius of 4′ (corresponding to 320 h_{50}^{-1} kpc) named region 1, region 2, and region 3. These regions are shown by blue circles in Figures 3, 4, and 5. Their characteristics are a hot faint region, a bright region with a southeast tail of central surface brightness excess, and a high-abundance region, respectively. The central positions of these peculiar regions are shown in Table 2. Each spectrum integrated in these regions was fitted with an absorbed thermal (Raymond-Smith) model, in order to confirm their characteristics of temperature and abundance. Results are also shown in Table 2. The temperature of region 1 and abundance of region 3 are 6.12 ± 0.18 keV and 0.58 ± 0.11 solar, respectively. Thus, region 1 indicates a significantly high temperature and region 3 has a significantly high abundance compared to the spectral parameters of the whole region. According to the spectral fitting, it is noted that another high-abundance region in the south ∼12′ from the center does not show a significantly high abundance. Therefore, we do not focus on this region.

On region 3 we performed further analysis to investigate the origin of the abundance excess. The redshift estimated from the center energy of the iron K line is $0.047^{+0.010}_{-0.004}$, which coincides with the average value obtained for the whole region of A3558, $0.051^{+0.005}_{-0.002}$, and the average redshift for

member galaxies, 0.0482 (Abell et al. 1989), within the error. Therefore, the newly detected high-abundance region is likely to be within the same gravitationally bound system as A3558. In order to know the extent of the metal-rich region, the abundances within the various integrated radii were estimated. Figure 6 shows the dependence of the abundance on the integrated radius. The region within a radius of 5′ has a significantly high abundance at a 90% confidence level. The significantly metal-rich region is thought to be within a radius of 4′, that is, 320 h_{50}^{-1} kpc, considering the point-spread function of the ASCA X-ray Telescope. The spectrum of region 3 is shown in the right panel of Figure 7. Because the abundance estimation is influenced by temperature, doubts are cast on the reliability of the high abundance. However, the temperature in this region, $5.17^{+0.27}_{-0.26}$ keV, is slightly lower than the most effective iron-emitting temperature, 6.6 keV. Therefore, even if the temperature is 6.6 keV, the abundance decreases to only 0.55 solar. Thus, the high abundance in this region is confirmed. It should be noted that both spectra in Figure 7 show high-energy tails. Although these structures are thought to be due to additional components, the spectral parameters do not suffer much from them.

It is thought to be clear that there is an additional metal-rich component at the same redshift as A3558. The excess iron abundance within a radius of 4′ is 0.3 ± 0.1 solar. However, because excess brightness in the whole energy band of 0.7–10 keV is not seen in Figure 5, it is thought that there is no significant additional gas cloud. Then, the mean gas density of this region is estimated to be ∼0.3×10^{-3} $h_{50}^{0.5}$ cm^{-3} on the assumption of a β-model gas distribution for the main cluster (core radius and β from Bardelli et al. 1996) with a central electron density of 2.3×10^{-3} $h_{50}^{0.5}$ cm^{-3}. The gas mass and the excess iron mass of the sphere within a radius of 320 h_{50}^{-1} kpc are estimated to be 8×10^{11} and 5×10^9 $h_{50}^{-2.5}$ $M_\odot$, respectively.

4. FIVE GALAXY CLUSTERS IN THE CORE REGION OF THE SHAPLEY SUPERCLUSTER

All ASCA data of A3562, SC 1329−313, SC 1327−312, and A3556 were analyzed with the same method as A3558. The whole obtained image of the core region of the supercluster is shown in Figure 1. Not all positions of the X-ray peaks of these five clusters are coincident with Figure 1 of Hanami et al. (1999) (the discrepancy of the peak position for SC 1327−312 is over 4′) but are consistent with the positions obtained from galaxy distribution (from the NASA/IPAC Extragalactic Database [NED]) within 1′. The temperature maps were not investigated by Hanami et al. (1999), except for SC 1329−313. Therefore, we estimated
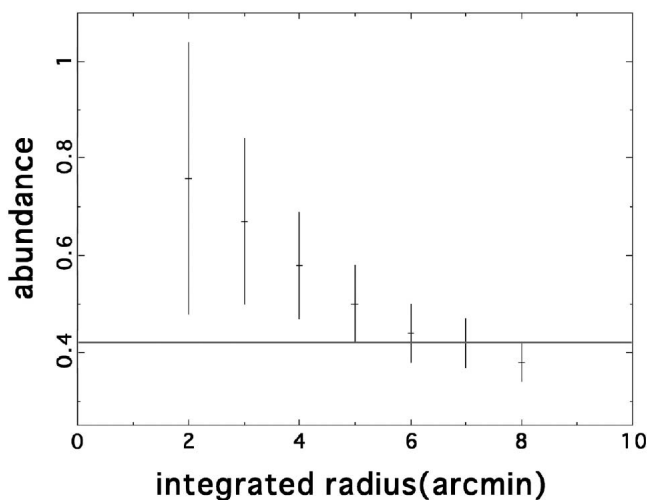
FIG. 6.—Relation between the integrated radius and the abundance of region 3. The line shows the upper limit of the average abundance of A3558.
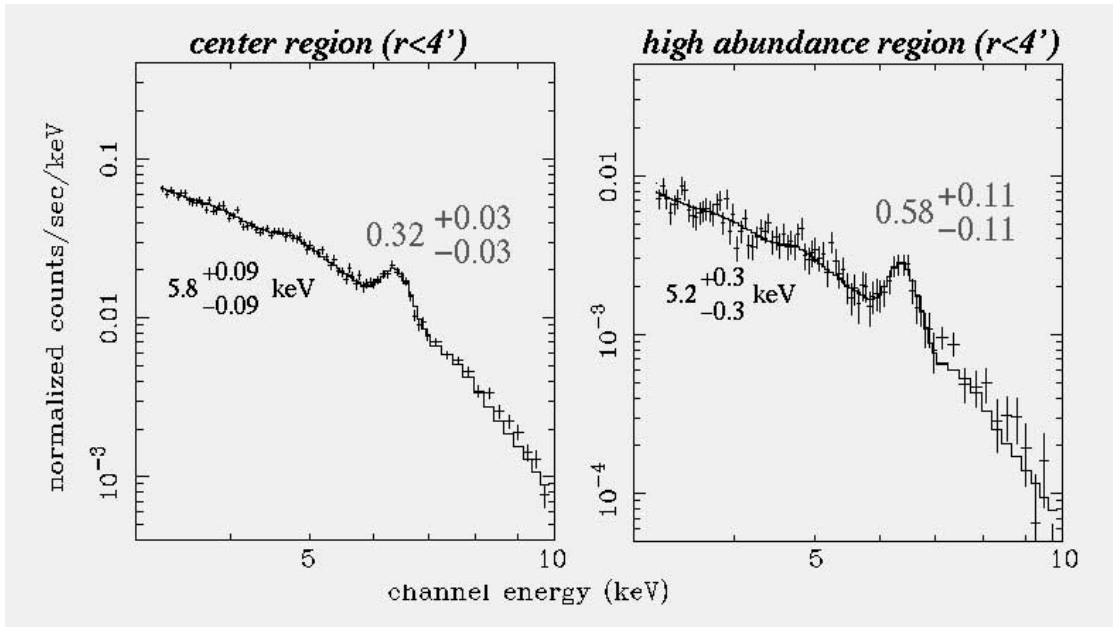
Fig. 7.—*ASCA* GIS spectra of the central region and high-abundance region within a radius of 4′. The temperature (keV) and abundance (solar) obtained by fittings with a thermal (Raymond-Smith) model are shown. *Right*: Spectrum of region 3. *Left*: Spectrum of the central region shown for comparison.

the maps for all member clusters with $4' \times 4'$ pixels. Three Abell clusters in the core region have asymmetric spatial distributions of the gas temperature, as shown in the hardness ratio map of Figure 8. For A3556 and A3562, the hardness ratio at the side toward A3558 seems to be higher than that toward the opposite side. Practically, spectra of the east and west sides of A3556 within a 12.′5 radius show that the temperature of the east side, $3.8^{+1.1}_{-0.7}$ keV, is higher than that of the west side, $2.6^{+0.5}_{-0.4}$ keV. The spectrum of the southwest region of A3562 within a radius of 12.′9 shows a temperature of $5.9^{+1.1}_{-0.7}$ keV, which tends to be higher than that of the northeast region, $4.6^{+0.8}_{-0.6}$ keV, although it is not significant. It is thought to be due to a cluster-cluster merging or a group infalling. On the other hand, the two poor clusters show relatively isotropic temperature distributions on the scale of $\sim 0.3 \, h_{50}^{-1}$ Mpc.

Gas temperature, abundance, and luminosity within a radius of 12′ for each cluster in the Shapley core are shown in Table 3. The total gravitational and gas mass of this core region can be estimated from these results and β-model parameters from those published (Bardelli et al. 1996; Ettori et al. 1997, 2000). The total gas mass is obtained to be $\sim 2 \times 10^{14} \, h_{50}^{-2.5} \, M_{\odot}$, and the total gravitational mass is $\sim 2 \times 10^{15} \, h_{50}^{-1} \, M_{\odot}$. Therefore, the mean gravitational density within a radius of $6.5 \, h_{50}^{-1}$ Mpc is 25 times larger than the critical density ρ_c.
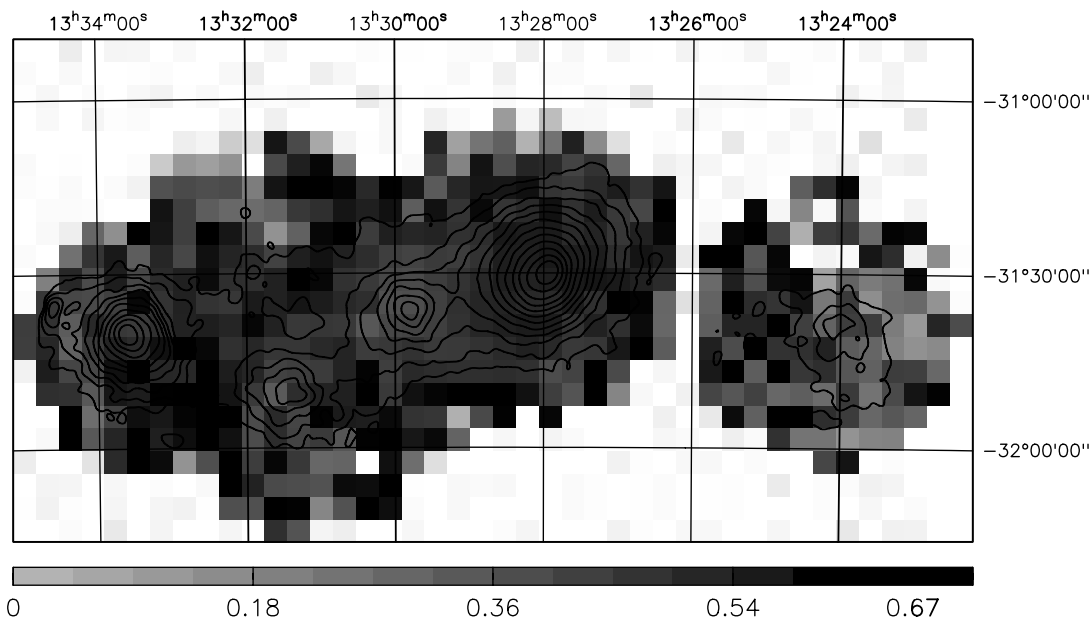
Fig. 8.—*ASCA* hardness ratio map of the core region in the Shapley supercluster. The hardness ratio is defined as the ratio of the 2.5–10 keV flux to the 0.7–2.5 keV flux. The superposed contours show the X-ray surface brightness for 0.7–10 keV and are the same as in Fig. 1. The pixel size is $4' \times 4'$.

TABLE 3
X-Ray Spectral Parameters of Five Galaxy Clusters

Parameter	A3562	SC 1329−313	SC 1327−312	A3558	A3556
Redshift	0.0490	0.0482	0.0495	0.0482	0.0479
kT (keV)............................	$5.04^{+0.23}_{-0.22}$	$4.22^{+0.25}_{-0.23}$	$3.65^{+0.14}_{-0.11}$	5.59 ± 0.06	$3.21^{+0.25}_{-0.24}$
Abundance (solar)	0.40 ± 0.08	$0.24^{+0.11}_{-0.10}$	0.32 ± 0.07	0.34 ± 0.02	$0.38^{+0.21}_{-0.18}$
L_X (10^{44} ergs s^{-1})................	$2.86^{+0.86}_{-0.07}$	$0.92^{+0.28}_{-0.03}$	$1.66^{+0.50}_{-0.04}$	$6.83^{+2.05}_{-0.04}$	$0.33^{+0.10}_{-0.03}$

Note.—These are estimated from 0.7–10 keV spectra within a radius of 12′ ($\sim$1 h_{50}^{-1} Mpc) of each target. The L_X is the luminosity of the 2–10 keV band.

Both the luminosity and temperature relation and the gravitational mass and temperature relation for these five clusters are consistent with those of the nearby clusters with a redshift of less than 0.1 investigated by Akimoto et al. (2001) and Matsumoto et al. (2000) within the deviations of their data. This result suggests that these five clusters are not peculiar clusters of galaxies.

5. DISCUSSION

The two-dimensional distributions of surface brightness, temperature, and abundance of A3558 indicate that this cluster has a high dynamical activity. This result is expected from the situation that this cluster resides at the center of a supercluster core with a high number density of member clusters. According to the distributions we investigated, this cluster is most probably suggested to at least have experienced mergings twice in the past and possibly to have had a recent group infalling.

The X-ray surface brightness distribution of A3558, showing elongation in the northwest and southeast direction, suggests that a merging of two large galaxy clusters with equal mass (major merger) has taken place along the major axis in the past, according to the results of an N-body simulation of head-on mergers (Roettiger, Loken, & Burns 1997). Although the spatial distribution of the temperature of A3558 is asymmetric, a hot region 3′ away from the cluster center northeastward does not spread out much, and the difference of temperature at each position within A3558 is small. Therefore, we think that it has been $\sim$5 Gyr since this major merging (Roettiger et al. 1997). In the case of the Coma Cluster, there is a large temperature fluctuation, even though it shows a smooth surface brightness (Watanabe et al. 1999). This focusing cluster is a contrary case to the Coma Cluster. It is not clear whether this merger had a small impact parameter or a large one. An N-body simulation of an offset merger for A3266 (Roettiger & Flores 2000) also gives a distribution of surface brightness that resembles A3558. Therefore, a scenario that a merging with a large impact parameter has taken place along the major axis in the past is not able to be rejected.

The characteristics of temperature and surface brightness in region 1 are discussed. They look like a cold front due to cluster merging reported by some authors based on *Chandra* observations (Markevitch et al. 2000; Vikhlinin et al. 2001; and so on). Considering the passage of time from the merging, it is difficult to think that these small-scale structures could have been formed by the above-described large-scale merger and still survive. It is plausible that after the large-scale merger occurred, the main cluster and a subcluster infalling from the northwest merged with a small impact parameter, and an area similar to a cold front was formed; however, no striking high- or low-temperature regions were made. According to the simulation of offset mergings with a mass ratio of 1 : 4 by Takizawa (2000), a bow shock and a merged cold core are seen for 0.25 Gyr after the closest contraction epoch of two merging clusters. At the end of the simulated time span (0.7 Gyr), although the distribution of surface brightness is still asymmetric, the fluctuation of temperature disappears. Therefore, it is thought that only less than 0.7 Gyr has passed after this small-scale merger. It is noted that the large elongated gas profile of A3558 would not have formed within 0.7 Gyr after the merging of one small-scale merger such as this, according to comparison in the cases of various mass ratios presented by Takizawa (2000) and Roettiger et al. (1997). The large ellipticity is likely to be due to the large-scale merging (major merger) mentioned above. Thus, the result that two cluster mergings happened is beyond a doubt.

On the origin of the high-abundance region (region 3), the most probable one of some possibilities is that it is a remnant of a merged subcluster core, which often shows abundance enhancement at an evolved stage. The diffusion time of iron is more than 15 Gyr. Therefore, the iron can persist for a long period in the remnant core after any dynamical event. Gas density fluctuations, on the other hand, fade away on the sound-crossing timescale, and any excess gas density is smeared out. In this way, regions with a typical size of a few hundred kiloparsecs with a significant iron excess but without a noticeable density excess can form.

In this cluster, the second small-scale merging with the passage of time of less than 0.7 Gyr cannot make the remnant of a merged core because this region is far from the cluster center. On the other hand, it is thought that the first major merging can form the iron remnant. After the first major merging, only the iron core can survive, since the diffusion time of iron is longer than $\sim$5 Gyr, that is, the passage of time after the large-scale merging.

To examine our scenario of a remnant of a merged cluster core with high metallicity, we constructed a simple toy model assuming an initial size of the merged cluster of 300 h_{50}^{-1} kpc, an abundance of 0.58 solar, and a central density of several 10^{-3} cm^{-3}, which is 10 times larger than the density of the ambient intracluster medium. After 0.3 Gyr, the radius of the core spreads at the sound speed of 1150 km s^{-1} and reaches 650 h_{50}^{-1} kpc. The gas density of the core comes to be the same value as that of the ambient intracluster medium, and then the brightness excess is smeared. The core size of iron ions, however, can increase to only 20 h_{50}^{-1} kpc within 0.3 Gyr, since iron ions expand through random walk with a thermal velocity of 130 km s^{-1}. The size of the

spread can be described by the product of the mean free path and square root of the number of collisions. The averaged number of collisions is 4.4. Thus, a region with no electron density excess, that is, no surface brightness excess, but with a high metal abundance will be able to be formed. After the formation, large-scale merging and mixing may have not been induced. Nonetheless, thermal conduction, dynamic viscosity, ram-pressure stripping, and Rayleigh-Taylor and Kelvin-Helmholtz instabilities make the time for an iron core to survive shorter, unless these processes are suppressed by magnetic fields.

Another suggestion is the existence of an active galactic nucleus (AGN) such as a type II Seyfert galaxy. The spatial distribution cannot determine whether the residual structure is caused by a point source or not, but the line center energy of iron $K\alpha$, that is, the redshift coincident within the error with the mean value of the overall region of the cluster within a radius of $12'$, and the time variability of this region are not detected significantly. No point source has been found in images of $ROSAT$, and no nonthermal component is needed to describe the $ASCA$ spectra. These facts do not support the idea of an AGN.

The other suggestion is the existence of a metal-rich group of galaxies. If there is a galaxy group that is binding the gas within $320\ h_{50}^{-1}$ kpc, it means that this region does not show strong interactions with A3558, and this idea is able to explain that the size of $320\ h_{50}^{-1}$ kpc is the typical size of groups of galaxies. If there is a group of galaxies, it has a gas mass of $8 \times 10^{11}\ h_{50}^{-2.5}\ M_\odot$ and an excess iron mass of $5 \times 10^9\ h_{50}^{-2.5}\ M_\odot$ within a sphere of this radius. The gas mass was derived assuming that the sphere has a uniform density. Because there is no clear electron density excess, the electron number density was set to be 0.0003 cm^{-3} at the center of this region. Thus, the gas mass was obtained. On the other hand, the gas mass within a column with a projected radius of $4'$ is $7 \times 10^{12}\ h_{50}^{-2.5}\ M_\odot$. Therefore, the iron mass is $1 \times 10^{10}\ h_{50}^{-2.5}\ M_\odot$ for an abundance of 0.58. The excess iron mass is 41% of the iron mass, that is, $5 \times 10^9\ h_{50}^{-2.5}\ M_\odot$. If the abundance for other regions of this sphere is 0.34, the sphere is then thought to have excess iron mass. These values are reasonable for a group of galaxies. For example, the radii of the X-ray extent of 78 groups and the intragroup medium masses of 24 groups are shown in Mulchaey et al. (1996). The iron abundance of galaxy groups varies significantly from group to group: 0–1 solar metallicity (Renzini 1997); therefore, the iron mass also varies between $\sim 10^8$ and $\sim 10^9\ h_{50}^{-2.5}\ M_\odot$.

In this paper, the iron K line is used, which is advantageous. There are 38 galaxies within the projected radius of $4'$ ($320\ h_{50}^{-1}$ kpc) according to the NED. Since not all of their redshifts are known, it is assumed that all are within this region. Because their total B-band luminosity is $2.3 \times 10^{11}\ L_{B\odot}$, the luminous mass is $2 \times 10^{12}\ M_\odot$ on the assumption that the mass-to-luminosity ratio is 8 for an elliptical galaxy. The ratio of the iron mass to the total optical luminosity of the galaxies is obtained to be $0.02\ M_\odot\ L_{B\odot}^{-1}$, which is also acceptable for galaxy groups. The ratio of galaxy groups varies over 0.0001–$0.02\ M_\odot\ L_{B\odot}^{-1}$ (Renzini 1997). Because not all of the 38 galaxies are members of the group, the total B-band luminosity and luminous mass are upper limits, and the ratio is a lower limit. Therefore, several other possible interpretations cannot be ruled out, such as bursts of star formation occurring because of group infalling, stars ejecting a large

amount of iron into the intragroup medium and then disappearing, or dust grains with condensed iron being evaporated.

Finally, the mean density of the core region in the Shapley supercluster is 25 times larger than the critical density. Although it is much smaller than needed to virialize, that is, 178 times critical density, it is larger than needed to decouple from the cosmic expansion and contract, that is, 5.6 times critical density (Peebles 1980). Therefore, the core region of the Shapley supercluster is on the way to contraction and is collapsing to form a virialized halo. However, because the characteristics of each member cluster in the core region are consistent with other typical nearby galaxy clusters, the core region of the Shapley supercluster is probably in the early phase of contraction. This scenario is supported by the fact that the core region is plotted at the right edge (the largest scale radius r_s and the lowest characteristic density δ_c) in Figure 4 of Sato et al. (2000).

6. CONCLUSIONS

The results of the $ASCA$ observations of five member clusters in the core region of the Shapley supercluster, mainly about A3558, are shown. The X-ray surface brightness distribution of A3558 is elongated in the northwest and southeast directions and is furthermore asymmetric to the axis. The temperature map shows that the central region within a radius of $1\ h_{50}^{-1}$ Mpc has a temperature gradient along the major axis. The range of temperature is 5.0–6.5 keV, and there are not extremely hot or cool regions. The obtained abundance map shows that the range of abundance is 0.3–0.5 solar and nearly isotropic. Spatial distributions of X-ray surface brightness, temperature, and abundance indicate a hot depression region $\sim 4'$ northwest (region 1), X-ray excess $\sim 4'$ southeast (region 2), and a metal-rich region within $\sim 320\ h_{50}^{-1}$ kpc, $12'$ southeast from the cluster center of A3558 (region 3).

The overall temperature and elongated distributions of surface brightness are thought to have arisen from a large-scale merging of two large galaxy clusters that occurred ~ 5 Gyr ago. The hot depression region (region 1) implies that a small-scale merging with the main cluster and a subcluster infalling from the northwest occurred less than 0.7 Gyr ago and after a large-scale merging. The anisotropic distributions of surface brightness and temperature indicate that mass infall along the major axis is dominant in the core region of the Shapley supercluster. As concerns the metal-rich region (region 3), it is probably the remnant of a core region in a galaxy cluster that merged ~ 5 Gyr ago. If it is not a remnant, it is possible that an infalling group of galaxies binding X-ray–emitting gas within $320\ h_{50}^{-1}$ kpc exists in this region. Thus, two mergers and a possible infalling of a galaxy group are suggested. It is thought that this cluster has a high dynamical activity due to the particular environment in the supercluster core.

Moreover, the gas temperature, abundance, luminosity, gas mass, and gravitational mass of the other four member clusters belonging in core region of the Shapley supercluster have been estimated. The values of these five galaxy clusters show the same correlations of L_X-kT and M_{gas}-kT relations as nearby galaxy clusters with a redshift of less than 0.1. Even though these five clusters of galaxies are in the highest density circumstance and some clusters show an anisotropic

temperature distribution, they have no differences with field clusters of galaxies; that is, the contribution of each interaction of the member clusters to overall spectral parameters is thought to be weak. The sum of the gravitational mass of the five galaxy clusters is $\sim 2 \times 10^{15}\ M_\odot$. There are no more significant X-ray sources bounding dark matter within the core region. Therefore, the mean density of the core region of the Shapley supercluster is about 25 times the critical density, which is smaller than 178 to start virializing but is larger than 5.5 to start contracting. The core region is just on the way to the contraction.

In order to make our discussion clear, observations with *Chandra*, *XMM*, and *Astro-E* II, which will be launched in 2005, are needed.

REFERENCES

Abell, G. O., Corwin, H. G., Jr., & Olowin, R. P. 1989, ApJS, 70, 1
Akimoto, F., Furuzawa, A., Yamashita, K., & Tawara, Y. 2001, in ASP Conf. Ser. 251, New Century of X-Ray Astronomy, ed. H. Inoue & H. Kunieda (San Francisco: ASP), 436
Anders, E., & Grevesse, N. 1989, Geochim. Cosmochim. Acta, 53, 197
Bardelli, S., Pisani, A., Ramella, M., Zucca, E., & Zamorani, G. 1998, MNRAS, 300, 589
Bardelli, S., Zucca, E., Malizia, A., Zamorani, G., Scaramella, R., & Vettolani, G. 1996, A&A, 305, 435
Bardelli, S., Zucca, E., Vettolani, G., Zamorani, G., Scaramella, R., Collins, C. A., & MacGillivray, H. T. 1994, MNRAS, 267, 665
Bardelli, S., Zucca, E., Zamorani, G., Moscardini, L., & Scaramella, R. 2000, MNRAS, 312, 540
Breen, J., Raychaudhury, S., Forman, W., & Jones, C. 1994, ApJ, 424, 59
Day, C. S. R., Fabian, A. C., Edge, A. C., & Raychaudhury, S. 1991, MNRAS, 252, 394
Dickey, J. M., & Lockman, F. J. 1990, ARA&A, 28, 215
Einasto, M., Tago, E., Jaaniste, J., Einasto, J., & Andernach, H. 1997, A&AS, 123, 119
Ettori, S., Bardelli, S., De Grandi, S., Molendi, S., Zamorani, G., & Zucca, E. 2000, MNRAS, 318, 239
Ettori, S., Fabian, A. C., & White, D. A. 1997, MNRAS, 289, 787
Hanami, H., Tsuru, T., Makishima, K., Yamauchi, S., Ikebe, Y., & Koyama, K. 1999, ApJ, 521, 90
Markevitch, M., & Vikhlinin, A. 1997, ApJ, 474, 84
Markevitch, M., et al. 2000, ApJ, 541, 542
Matsumoto, H., Tsuru, T. G., Fukazawa, Y., Hattori, M., & Davis, D. S. 2000, PASJ, 52, 153
Metcalfe, N., Godwin, J. G., & Peach, J. V. 1994, MNRAS, 267, 431
Mulchaey, J. S., Davis, D. S., Mushotzky, R. F., & Burstein, D. 1996, ApJ, 456, 80
Peebles, P. J. E. 1980, The Large-Scale Structure of the Universe (Princeton: Princeton Univ. Press)
Raychaudhury, S., Fabian, A. C., Edge, A. C., Jones, C., & Forman, W. 1991, MNRAS, 248, 101
Renzini, A. 1997, ApJ, 488, 35
Roettiger, K., & Flores, R. 2000, ApJ, 538, 92
Roettiger, K., Loken, C., & Burns, J. O. 1997, ApJS, 109, 307
Sarazin, C. L. 1988, Cooling Flows in Clusters and Galaxies (NATO ASIC Proc. 229; Dordrecht: Kluwer)
Sato, S., Akimoto, F., Furuzawa, A., Kumai, Y., Tawara, Y., & Watanabe, M. 2000, ApJ, 537, L73
Shapley, H. 1930, Hvar. Obs. Bull., 874, 9
Takizawa, M. 2000, ApJ, 532, 183
Vikhlinin, A., Markevitch, M., & Murray, S. S. 2001, ApJ, 551, 160
Watanabe, M., Yamashita, K., Furuzawa, A., Kunieda, H., & Tawara, Y. 2001, PASJ, 53, 605
Watanabe, M., Yamashita, K., Furuzawa, A., Kunieda, H., Tawara, Y., & Honda, H. 1999, ApJ, 527, 80